Dynamic Harmonic Domain Transmission Line Modeling for Transients

J. Jesus Chavez, Abner Ramirez, and J. Luis Naredo

Abstract—Harmonics have become a relevant topic as the number of nonlinear elements and electronic devices connected to power systems is increasing constantly. This paper presents a methodology for the modeling of single-phase transmission lines interfaced with nonlinear loads. It is intended for transient analysis and special emphasis is put on the harmonic content of the propagating waveforms through the dynamic harmonic domain (DHD) technique.

Keywords: Dynamic harmonic domain, electromagnetic transients, harmonics, switching maneuvers, transmission line, time-varying systems.

I. Introduction

TRADITIONALLY, transmission lines are modeled either in the frequency domain or in the time domain, a partial list of important developments in this area is [1]-[9]. By using any of these models one can obtain voltage or current traveling waves as functions of time. Nevertheless, one could be interested in analyzing the harmonic content of such waves, especially when nonlinear loads or electronic devices are connected to the lines being analyzed. Moreover, the consideration of harmonics in a transmission line/nonlinear load system is desirable when assessing ferroresonance conditions [10].

In this paper we model the transmission line by the traveling wave approach combined with the Dynamic Harmonic Domain (DHD) technique [11]. The latter consists on representing a time-varying quantity by a Fourier series whose coefficients are allowed to vary slowly [12], [13].

Potential applications of the proposed technique are in the areas of power quality studies and of ferroresonance analysis. Power quality indices are calculated here to illustrate the application of the proposed methodology to the power quality area. The link between the HD and ferroresonance analysis can be seen in [14] and, since it is beyond the scope of the present work, it is relegated to a forthcoming paper.

Accounting for enough harmonics, the DHD technique permits to follow in a step-by-step fashion the voltage/current harmonics behavior with respect to time in a precise manner. This way, DHD avoids the well-known errors intrinsically involved in traditional techniques such as the Windowed Fast Fourier Transform (WFFT).

Although FFT-based methods are efficient in stationary conditions, they loss accuracy under time-varying conditions [15]. See [15]-[18] for a detailed analysis of such errors, i.e., leakage, picket-fence, etcetera.

The paper is organized as follows. In section II the basic definitions of the DHD technique are presented. Section III describes the DHD modeling of transmission lines, of nonlinear loads and of their interconnection. Numerical results are presented in Section IV.

II. DHD BASIC THEORY

A. Theory

Without loss of generality consider the Linear Time Periodic (LTP) system for the scalar case

$$\dot{x} = a_p x + b_p u , \tag{1a}$$

$$y = c_p x + d_p u , \tag{1b}$$

where subscript p stands for *time-periodic*; for instance a_p is defined as

$$a_p = a_{-h} e^{-jh\omega_o t} + \cdots + a_o + \cdots + a_h e^{jh\omega_o t} , \tag{2}$$

with h representing the highest harmonic and ω_o the fundamental frequency. The state representation (1) is expressed in the DHD as

$$\dot{X} = (A - S)X + BU , \tag{3a}$$

$$Y = CX + DU , \tag{3b}$$

where the variables are now complex vectors with time-varying coefficients, e.g.,

$$X = [x_{-h}(t) \quad \cdots \quad x_o(t) \quad \cdots \quad x_h(t)]^T , \tag{4a}$$

where T denotes transpose, S is called the operational matrix of differentiation defined by [13], [19]

$$S = diag\{-jh\omega_o, \ldots, -j\omega_o, 0, j\omega_o, \ldots, jh\omega_o\}, \tag{4b}$$

J.J. Chavez and A. Ramirez are with CINVESTAV-Guadalajara, Mexico (e-mails: (jchavez@gdl.cinvestav.mx, abner.ramirez@cts-design.com), J.L. Naredo is with CINVESTAV-Queretaro, Mexico (e-mail: jlnaredo@qro.cinvestav.mx)

and matrix A (as well as B, C and D) has Toeplitz structure

$$A = \begin{bmatrix} a_o & a_{-1} & \cdots & a_{-h} & & \\ a_1 & a_o & \ddots & & a_{-h} & \\ \vdots & \ddots & \ddots & \ddots & & \vdots \\ a_h & & \ddots & a_o & a_{-1} \\ & a_h & \cdots & a_1 & a_o \end{bmatrix}. \tag{4c}$$

By comparing (1) and (3) one can observe that the LTP system has been transformed into a Linear Time Invariant (LTI) one through the DHD. Moreover, the steady state of the system is easily obtained by setting to zero the derivatives in (3), thus yielding

$$X = (S - A)^{-1} BU , \tag{5a}$$

$$Y = CX + DU , \tag{5b}$$

Hence, the evolution of the harmonic content, *i.e.*, with respect to time, can be obtained from (3) and the corresponding instantaneous values are calculated by assembling a Fourier series as in (2).

B. Illustrative example

Consider the signal shown in Fig. 1 and given by

$$x(t) = \gamma[\cos(\omega_o t) + 0.3\cos(3\omega_o t + \pi/10) + 0.1\cos(5\omega_o t + \pi/5)], \tag{6a}$$

where ω_o is the power frequency in rad/s and $\gamma = 1 - 0.5e^{-20t}$. The corresponding harmonic vector (showing only the odd harmonics) is

$$X = \begin{bmatrix} x_{-5} \\ x_{-3} \\ x_{-1} \\ x_1 \\ x_3 \\ x_5 \end{bmatrix} = \frac{\gamma}{2} \begin{bmatrix} 0.1e^{-j\pi/5} \\ 0.3e^{-j\pi/10} \\ 1 \\ 1 \\ 0.3e^{j\pi/10} \\ 0.1e^{j\pi/5} \end{bmatrix}. \tag{6b}$$

From (6b) one can notice that the harmonic coefficients are time dependent. This is shown in Fig. 2.

Additionally, for comparison purposes Fig. 2 presents the results yielded by the WFFT. For this example, the original signal given by (6a) has 1280 points and a sliding window with 128 points (sampling rate of 7.68 kHz) is used. In order to diminish the leakage error, each windowed data is multiplied by the Hanning window. Notice that the WFFT follows closely the exact values of the harmonics given by the DHD; the latter lacking the intrinsic errors of the former.
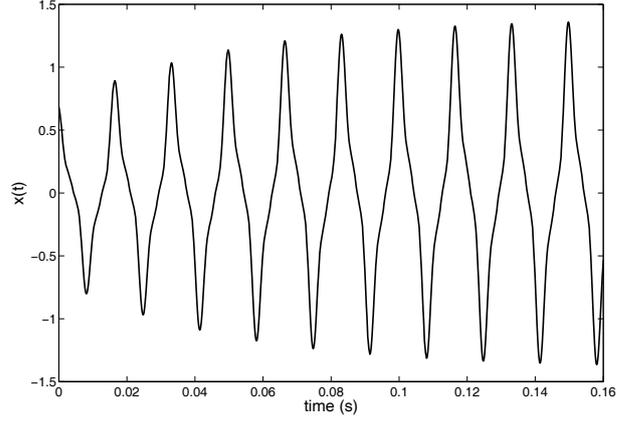
Fig. 1. Time-varying signal with harmonics
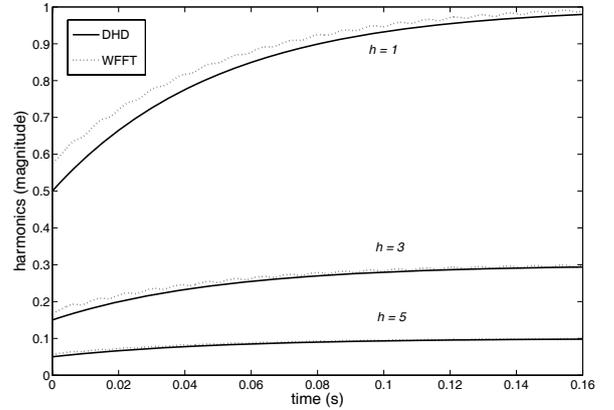
Fig. 2. Harmonic dynamics for time-varying signal

III. TRANSMISSION LINE-NONLINEAR LOAD IN THE DHD

A. Propagation Equations

Consider the reference directions for the transmission line depicted in Fig. 3. The relations between the incident current, I', and the reflected current, I'', in the frequency domain are

$$I'_m = H I''_n , \tag{7a}$$

$$I'_n = H I''_m , \tag{7b}$$

where H represents the propagation function [5]. On approximating H by rational functions [8] we can express (7b) as

$$I'_n = [C_1(sI - A_1)^{-1} B_1] I''_m . \tag{8a}$$

In (8a) the set of poles (k poles), obtained from the rational fitting, are contained in the diagonal matrix A_1 of dimensions $k \times k$; the column vector B_1 ($k \times 1$) has all entries equal to 1 and the residues of the realization are contained in the row vector C_1 ($1 \times k$). From (8a) we define

$$X_1 = (sI - A_1)^{-1} B_1 I''_m , \tag{8b}$$

2

The corresponding state-space realization for (8b) becomes

$$\dot{x}_1 = A_1 x + B_1 i_m'' , \qquad (8c)$$

Using a similar procedure for node m, the state space realization for (7a) is straightforward to obtain. The state space realization for the two line nodes is thus

$$\begin{bmatrix} \dot{x}_1 \\ \dot{x}_2 \end{bmatrix} = \begin{bmatrix} A_1 & \\ & A_1 \end{bmatrix} \begin{bmatrix} x_1 \\ x_2 \end{bmatrix} + \begin{bmatrix} B_1 & \\ & B_1 \end{bmatrix} \begin{bmatrix} i_n'' \\ i_m'' \end{bmatrix} , \qquad (9a)$$

$$\begin{bmatrix} i_m' \\ i_n' \end{bmatrix} = \begin{bmatrix} C_1 & \\ & C_1 \end{bmatrix} \begin{bmatrix} x_1 \\ x_2 \end{bmatrix} , \qquad (9b)$$

In (9), the reflected currents i_n'' and i_m'' are calculated at time $t-\tau$, being τ the travel time. In the DHD, (9) becomes

$$\begin{bmatrix} \dot{X}_1 \\ \dot{X}_2 \end{bmatrix} = \begin{bmatrix} A_1 - S' & \\ & A_1 - S' \end{bmatrix} \begin{bmatrix} X_1 \\ X_2 \end{bmatrix} + \begin{bmatrix} B_1 \Gamma & \\ & B_1 \Gamma \end{bmatrix} \begin{bmatrix} I_n' \\ I_m' \end{bmatrix} , \quad (10a)$$

$$\begin{bmatrix} I_m' \\ I_n' \end{bmatrix} = \begin{bmatrix} C_1 & \\ & C_1 \end{bmatrix} \begin{bmatrix} X_1 \\ X_2 \end{bmatrix} , \qquad (10b)$$

Now, in (10) we have the following matrix definitions with corresponding dimensions shown inside round parenthesis:

$$A_1 = diag\{a_1 I_h, a_2 I_h, \cdots, a_k I_h\} \quad (kh \times kh) , \qquad (11a)$$

$$S' = diag\{S, S, \cdots, S\} \quad (kh \times kh) , \qquad (11b)$$

$$B_1 = \begin{bmatrix} I_h & I_h & \cdots & I_h \end{bmatrix}^T \quad (kh \times h) , \qquad (11c)$$

$$C_1 = \begin{bmatrix} c_1 I_h & c_2 I_h & \cdots & c_k I_h \end{bmatrix} \quad (h \times kh) , \qquad (11d)$$

$$\Gamma' = diag\{\Gamma, \cdots, \Gamma\} \quad (kh \times kh) , \qquad (11e)$$

In (11), I_h corresponds to the identity matrix of dimensions $h \times h$ and the time delay is taken into account by

$$\Gamma = diag\{e^{jh\omega_o\tau}, \cdots, 1, \cdots e^{-jh\omega_o\tau}\} . \qquad (11f)$$

One can observe from (10) that the dimension of the dynamic system has been increased h times. Although the computational advantages of (10) compared to (9) are questionable, the former permits us to follow the dynamics of any harmonic along the observation time.
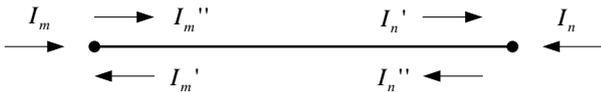
Fig. 3. Transmission line reference directions

B. Node Equations

In addition to the propagation equations, we have in the frequency domain the terminals relations (see Fig. 3)

$$Y_c V_m - I_m = 2 I_m' , \qquad (12a)$$

$$Y_c V_n - I_n = 2 I_n' . \qquad (12b)$$

Assuming that the voltage at node m is known, the time domain realization for (12a) is (Y_c being fitted with rational functions)

$$\dot{x}_3 = A_2 x_3 + B_2 v_m , \qquad (13a)$$

$$i_m = C_2 x_3 + D_1 v_m - 2 i_m' , \qquad (13b)$$

with their corresponding DHD counterpart given by

$$\dot{X}_3 = (A_2 - S') X_3 + B_2 V_m , \qquad (14a)$$

$$I_m = C_2 X_3 + D_1 V_m - 2 I_m' , \qquad (14b)$$

where A_2, B_2, C_2, and D_1 are defined in accordance with (11a)-(11)e. The reflected current is then updated with

$$I_m'' = I_m' + I_m . \qquad (15)$$

Similarly, from (12b) for node n we have in the DHD

$$\dot{X}_4 = (A_2 - S') X_4 + B_2 V_n , \qquad (16a)$$

$$I_n = C_2 X_4 + D_1 V_n - 2 I_n' . \qquad (16b)$$

Considering a nonlinear load in parallel with a resistive load connected to node n (as shown in Fig. 4), the terminal voltage v_n can be eliminated from (16) by application of Kirchhoff Currents Law. First, let us assume that the total load current (linear and nonlinear) is given in the time domain by

$$i_n = -\alpha\varphi - \beta\varphi^p - v_n / R ; \qquad (17a)$$

with its counterpart in the DHD given by

$$I_n = -\alpha\Phi - \beta\Phi^p - V_n / R ; \qquad (17b)$$

where, for the nonlinear load we have assumed a current/flux polynomial relation and now in (17b) the power p is related with a convolution operation (see Appendix A).
Then, substitution of (17b) into (16b) gives

$$V_n = k(-\alpha\Phi - \beta\Phi^{(p)} - C_2 X_4 + 2 I_n') , \qquad (18)$$

where $k = R/(1 + R D_1)$. Next, substituting (18) into (16a) and taking into account the voltage/flux relation in the DHD

$$\dot{\Phi} + S\Phi = V_n , \qquad (19)$$

one obtains the final relations for node n as follows:

$$\begin{bmatrix} \dot{X}_4 \\ \dot{\Phi} \end{bmatrix} = \begin{bmatrix} A_2 - S' - k B_2 C_2 & -k B_2 (\alpha + \beta\Phi^{(p-1)}) \\ -k C_2 & -S - k(\alpha + \beta\Phi^{(p-1)}) \end{bmatrix} \begin{bmatrix} X_4 \\ \Phi \end{bmatrix} + 2k \begin{bmatrix} B_2 \\ I_h \end{bmatrix} I_n' , \quad (20a)$$

$$I_n = \frac{1}{R}\Big[kC_2\ (k-R)(\alpha + \beta\Phi^{(p-1)})\Big]\begin{bmatrix} X_4 \\ \Phi \end{bmatrix} - \frac{2k}{R}I_n' . \quad \text{(20b)}$$

Finally, after calculating I_n from (20), the reflected current is updated with

$$I_n'' = I_n' + I_n . \quad \text{(21)}$$

In the case of a network with several transmission lines, the procedure described above could be used [14]. The incident currents are calculated for each line using an expression similar to (10). The solution for each load node can be calculated by using the nodal elimination as in (20). Finally, the reflected currents are updated.
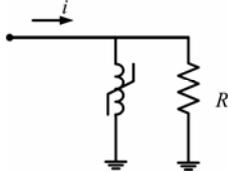
Fig. 4. Nonlinear/linear load

IV. EXAMPLE

Consider the network shown in Fig. 5. It consists of three transmission lines having a resistive load at bus 2 (Z_1) and identical linear/nonlinear loads (as specified by (17a) and depicted in Fig. 4) that are connected at buses 3 and 4 with $R = 1 \times 10^3$ ohms, $\alpha = 1/10$, and $\beta = 5 \times 10^5$. For simplicity, the lines are considered identical with 100 km of length, conductor radius equal to 0.0254 m, 15 m height, and earth resistivity equal to 100 ohm-m.

Initially, zero initial conditions are assumed with sw_1 open, sw_2 and sw_3 closed. Then, at $t = 0$ sw_1 is closed and at $t = 0.023$ s sw_2 is opened and it remains opened during the whole observation time. The results from the DHD are compared with those obtained from the direct simulation of the system of nonlinear equations in the time domain (labeled as TD in Figs. 6-8) using a predictor-corrector type method.

For this example, we have taken a polynomial of order $p = 3$ for (17a) and 17 harmonics, positive and negative, are being considered.
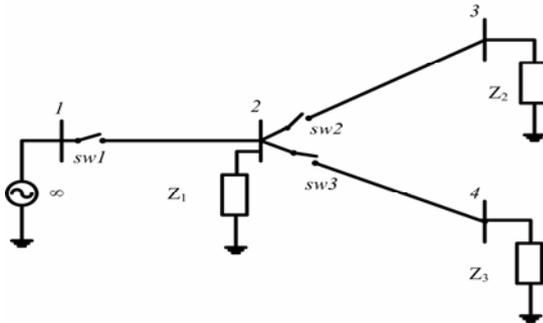
Fig. 5. Network configuration with four buses

a)

b)
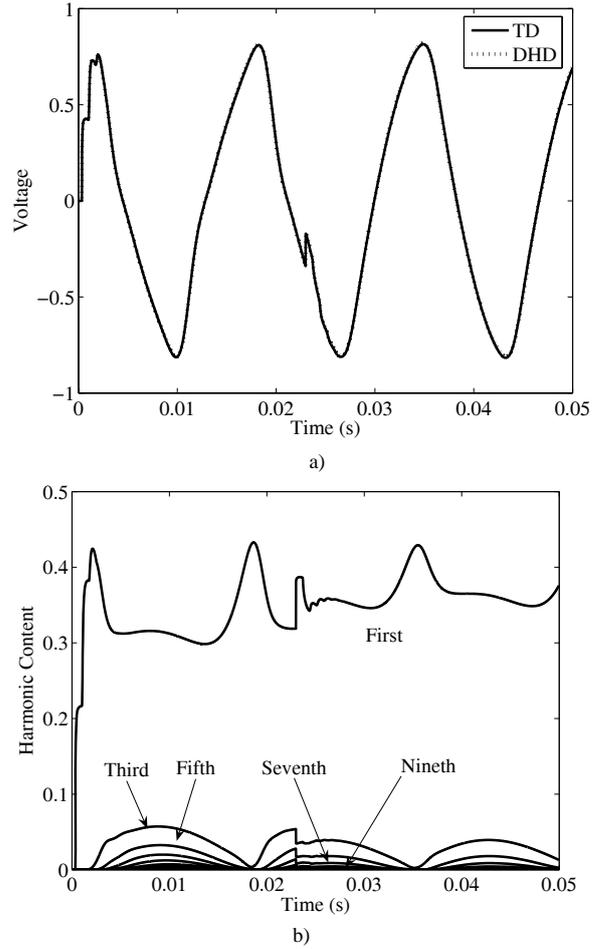
Fig. 6. a) Voltage and its b) harmonic content at bus 2

Fig. 6 shows the instantaneous voltage and its harmonic content for bus 2 where the difference (in the voltage waveform) between the simulation of the original ODEs and the one from the DHD is almost unnoticeable. One can notice from Fig. 6a the transient waveforms when closing $sw1$ and when opening $sw2$. Accordingly, Fig. 6b shows the harmonics behavior during the whole observation time. In Fig. 6b the harmonics oscillate with power frequency. The attenuation of these oscillations is not noticeable given the very low damping of the system under study. If there was a very large damping the harmonic plots would become horizontal lines in Fig. 6b. This would denote that the steady state was reached very fast.

The voltage, load current and the corresponding harmonics at bus 4 are shown in Figs. 7 and 8. Similar observations can be concluded as in the preceding paragraph.

4

a)

b)
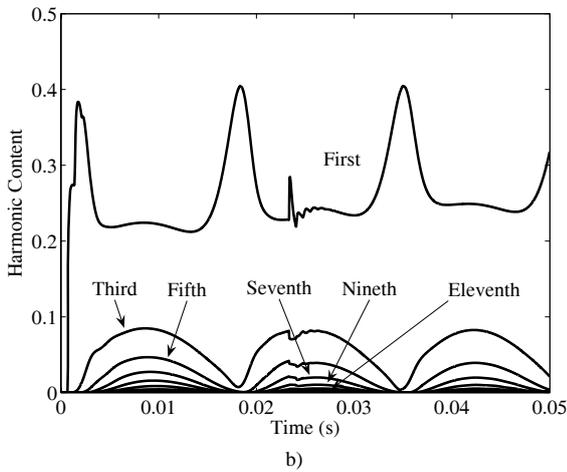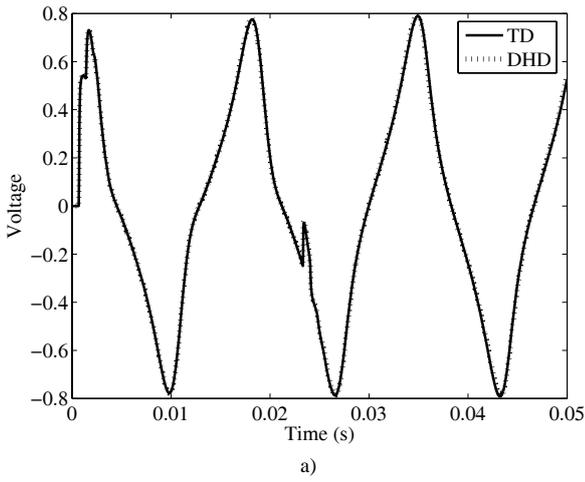
Fig. 7. a) Voltage and its b) harmonic content at bus 4

It should be mentioned that although the direct time domain (TD) simulation takes much less time than the DHD, the harmonic dynamics needs an additional processing procedure to be followed, such as using WFFT.

a)

b)
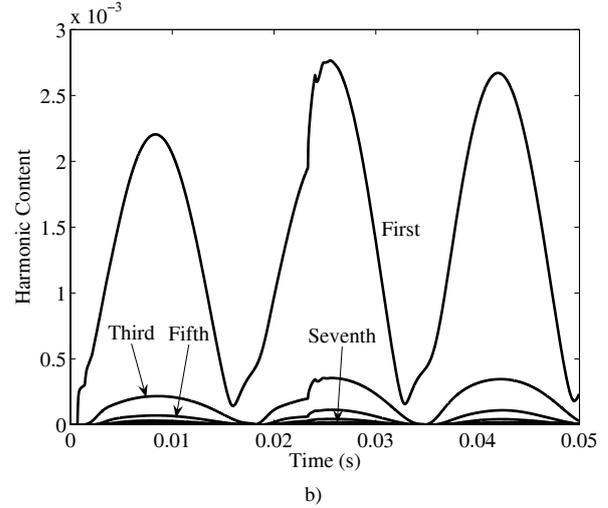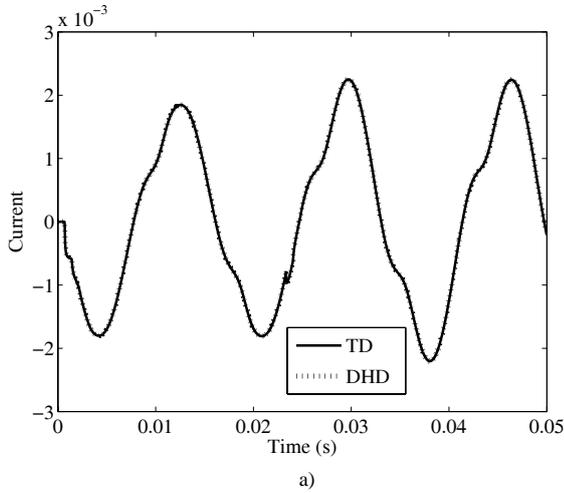
Fig. 8. a) Load current and its b) harmonic content at bus 4

In Fig. 9 the active, apparent, and distortion powers for bus 4 are presented. We have used the expressions given in [13] for this calculations. The remaining of the power quality indices can be calculated using those formulae but are not shown here.

a)

b)

5
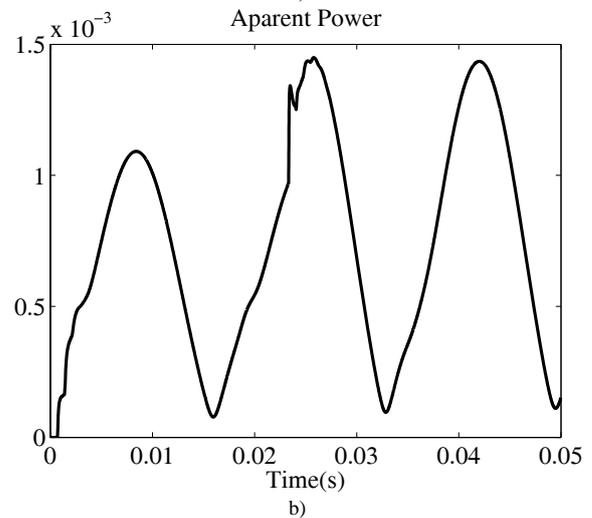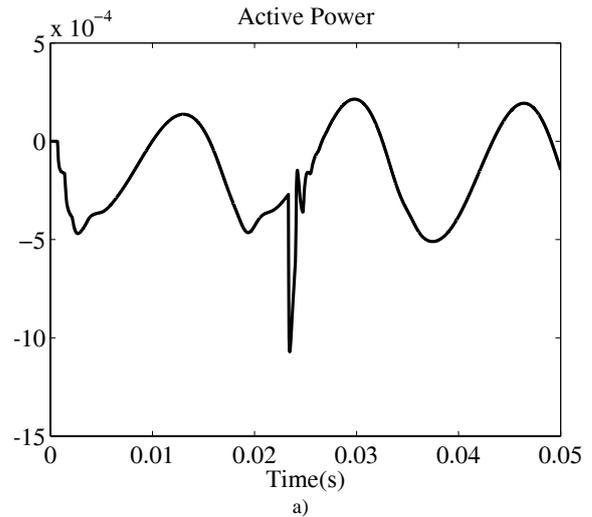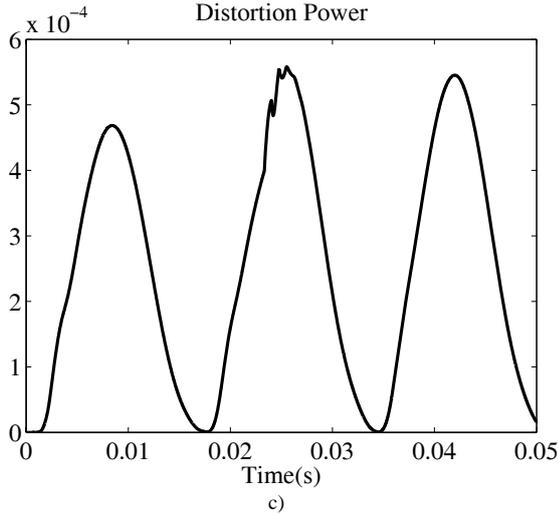
Fig. 9. a) Active, b) Apparent, and c) distortion powers at bus 4

V. CONCLUSIONS

In this paper a methodology for handling a system consisting of transmission lines and nonlinear loads has been proposed. The methodology takes aim into the dynamic harmonic domain which permits to follow step-by-step the harmonic evolution with respect to time. Its validation is made here through the original ODEs. Although the proposed methodology has been described for single-phase lines, it can be extended for the multi-phase case in a straightforward manner. The proposed technique is intended for contributing in the study of harmonics in transient state.

VI. APPENDIX A (NONLINEAR LOAD IN THE DHD)

Consider the time domain representation of a nonlinear load given by the flux/current relation $i(t) = f(\varphi)$. Such nonlinear relation can be expressed in general as a polynomial of the type [14]

$$i = \alpha\varphi + \beta\varphi^p . \qquad (22)$$

In the DHD, we have a relation similar to (22) where i and φ now become harmonic vectors as in (4a). The term φ^p is calculated by harmonic convolution (denoted here with the symbol $\otimes$) [13]. For instance,

$$\Phi^2 = \Phi \otimes \Phi = T_o\Phi , \qquad (23a)$$

where:

$$T_o = \begin{bmatrix} \varphi_o & \varphi_{-1} & \cdots & \varphi_{-p} & & \\ \varphi_1 & \varphi_o & \ddots & & \varphi_{-p} & \\ \vdots & \ddots & \ddots & \ddots & & \vdots \\ \varphi_p & & \ddots & \varphi_o & \varphi_{-1} \\ & \varphi_p & \cdots & \varphi_1 & \varphi_o \end{bmatrix} . \qquad (23b)$$

It can easily be shown that

$$\Phi^p = \Phi \otimes \cdots \otimes \Phi = T_o^{p-1}\Phi . \qquad (23c)$$

VII. REFERENCES

[1] A. Semlyen, A. Dabuleanu, "Fast and Accurate Switching Transient Calculations on Transmission Lines with Ground Return Using Recursive Convolutions", *IEEE Trans. on Power Apparatus and Systems*, vol. PAS-94, pp. 561-571, March/April 1975.

[2] J. R. Marti, "Accurate Modeling of Frequency-Dependent Transmission Lines in Electromagnetic Transient Simulations", *IEEE Trans. on Power Apparatus and Systems*, vol. PAS-101, no. 1, pp. 147-157, January 1982.

[4] T. Noda, N. Nagaoka, and A. Ametani, "Phase Domain Modeling of Frequency-Dependent Transmission Lines by Means of an ARMA Model", *IEEE Trans. on Power Delivery*, vol. 11, no. 1, pp. 401-411, January 1996.

[5] F. J. Marcano and J. R. Marti, "Idempotent Line Model: Case Studies", *Proc. of the International Conference on Power Systems Transients*, pp., Seattle, Washington, June 1997.

[6] H. V. Nguyen, H. W. Dommel, and J. R. Marti, "Direct Phase-Domain Modelling of Frequency-Dependent Overhead Transmission Lines", *IEEE Trans. on Power Delivery*, vol. 12, no. 3, pp. 1335-1342, July 1997.

[7] F. Castellanos and J. R. Marti, "Full Frequency-Dependent Phase-Domain Transmission Line Model", *IEEE Trans. on Power Systems*, vol. 12, no. 3, pp. 1331-1339, August 1997.

[8] B. Gustavsen and A. Semlyen, "Combined Phase Domain and Modal Domain Calculation of Transmission Line Transients Based on Vector Fitting", *IEEE Trans. Power Delivery*, vol. 13, no. 2, pp. 596-604, April 1998

[9] A. Morched, B. Gustavsen, and M. Tartibi, "A Universal Model for Accurate Calculation of Electromagnetic Transients on Overhead Lines and Underground Cables", *IEEE Trans. on Power Delivery*, vol. 14, no. 3, pp. 1032-1037, July 1999.

[10] TF on Slow Transients, "Modeling and Analysis Guidelines for Slow Transients–Part III: The Study of Ferroresonance", *IEEE Trans. on Power Delivery*, vol. 15, no. 1, pp. 255-265, January 2000.

[11] J. Jesus Rico, Manuel Madrigal and Enrique Acha, "Dynamic Harmonic Evolution Using the Extended Harmonic Domain," *IEEE Trans. Power Delivery*, vol. 18, pp. 587-594, Apr. 2003.

[12] S.R. Sanders, J.M. Noworolski, X.Z. Lui, and G.C. Verghense, "Generalized Averaging Method for Power Conversion Circuits", *IEEE Trans. on Power Electron.*, vol. 6, pp. 251-259, Apr. 1991.

[13] E. Acha, and M. Madrigal *Power Systems Harmonics*, England: Wiley, 2001.

[14] Abner Ramirez, Adam Semlyen and Reza Iravani "Harmonic Domain Characterization of the Resonant Interaction between Generator and Transmission Line," *IEEE Trans. Power Delivery*, vol. 20, pp. 1753-1762, Apr. 2005.

[15] M. Karimi-Ghartmani and R. Iravani, "A Nonlinear Adaptive Filter for Online Signal Analysis in Power Systems: Applications", *IEEE Trans. on Power Delivery*, vol. 20, no. 1, January 2005.

[16] G.T. Heydt P.S Fjeld, C.C. Liu, D. Pierce, L. Tu, and G. Hensley, "Aplications of the Windowed FFT to Electric Power Quality Assessment", *IEEE Trans. on Power Delivery*, vol. 14, no. 4, pp. 1411-1416, October 1999.

[17] S. Qian and D. Chen, "Joint time-frequency analysis," IEEE Signal Processing Mag. vol 16, pp. 52-67, 1999.

[18] H. Qian, R. Zhao, and T. Chen, "Interharmonics Analysis Based on Interpolating Windowed FFT Algorithm", *IEEE Trans. on Power Delivery*, soon to appear.

[19] Taku Noda, Adam Semlyen and Reza Iravani "Enterely Harmonic Domain Calculation of Multiphase Nonsinusoidal Steady State," *IEEE Trans. Power Delivery*, vol. 19, pp. 1368-1377, July. 2004.

6

VIII. BIOGRAPHIES

J. Jesus Chavez received his B.Sc. from the University of Guadalajara, Guadalajara, Mexico, in 2003, the M.A.Sc. from the Center for Research and Advanced Studies of Mexico (CINVESTAV) Campus Guadalajara, in 2006.
He is currently pursuing his Ph.D degree at CINVESTAV. His interests are electromagnetic transient analysis in power systems and the dynamic harmonic domain applying to electronics devices in power systems.

Abner Ramirez received his B.Sc., M.A.Sc. and Ph.D. from University of Guanajuato, Mexico, in 1996, University of Guadalajara, Mexico, in 1998 and from the Center for Research and Advanced Studies of Mexico (CINVESTAV) Campus Guadalajara, in 2001, respectively. He was a postdoctoral fellow in the Department of Electrical and Computer Engineering of the University of Toronto from November 2001 to January 2005. Currently, he is a Professor at CINVESTAV-Guadalajara. His interests are electromagnetic transient analysis in power systems and numerical analysis of electromagnetic fields.

Jose Luis Naredo received the Electrical and Mechanical Engineering degree from Universidad Anahuac, Mexico, in 1983, and the M.A.Sc. and Ph.D. degrees from the University of British Columbia, Canada, in 1987 and 1992, respectively. In May 1997, he joined the Faculty of the Center for Research and Advanced Studies of Mexico (CINVESTAV) Campus Guadalajara. Since February 2005 he is the director of Cinvestav, Campus Queretaro. His research interests include electromagnetic transient analysis in transmission lines, telecommunications in power systems and digital protections.